January 2007

Technical Memorandum: UCPRC-TM-2007-04

Interim Assessment of Expected Structural Life of Pre-Cast Concrete Pavement Slabs with HVS Testing

Authors:
Erwin Kohler, Hechter Theyse, and Louw du Plessis

Work Conducted as part of Partnered Pavement Research Center Strategic Plan Element No. 4.17: HVS testing of pre-cast PCC panels in District 8

PREPARED FOR:

California Department of Transportation
(Caltrans)
Division of Research and Innovation

PREPARED BY:

University of California
Pavement Research Center
UC Davis and Berkeley

DOCUMENT RETRIEVAL PAGE		Technical Memorandum: UCPRC-TM-2007-04
Title: Interim Assessment of Expected Structural Life of Pre-Cast Concrete Pavement Slabs		
Authors: Erwin Kohler, Hechter Theyse, and Louw du Plessis		
Prepared for: Caltrans Division of Research and Innovation and Caltrans District 8	**FHWA No.:** CA081087A	**Date**: January 2007
Strategic Plan Element No: 4.17	**Status:** Final, approved	**Version No.:** Stage 6

Abstract:

This document presents partial results of the HVS Test 597FD. The results are partial because they comprise only the HVS test in dry conditions, and not the continuation of the test performed with the addition of water at the joints for accelerated damage. The first draft of this documented was submitted to Caltrans in October 2005. The test had taken place between June 8 and September 20, 2005. Almost 1.24 millions wheel load repetitions were applied to the pavement during that period. Load levels of 60, 80, 120, and 150kN were progressively applied through an aircraft tire with 1,400kPa of pressure (209psi). Structural corner cracks were first observed at about 762,000 repetitions and were fully developed at 845,000 load repetitions. A significant increase in the joint deflection was observed, but it did not result in any terminal failures of the pavement.

Given the design of the pre-cast PCC pavement tested at the San Bernardino test site, the tight control over the construction process, and the favorable HVS test conditions, no premature failure is anticipated with the use of the pre-cast PCC pavement on actual rehabilitation projects. The ultimate structural capacity of the system will probably exceed 40 million ESALS. The structural capacity of the system will, however, have to be determined for a range of support and environmental conditions before it can be used with absolute certainty.

Keywords:

Pre-cast concrete slabs, Super-Slab, Heavy Vehicle Simulator, HVS, Experimental pavement section, Thermal Curling, Pavement Responses, Accelerated Pavement Testing, Instrumented Slabs

Proposals for implementation:

Overnight opening to traffic in the un-grouted condition is acceptable for the Super-Slab System

Related documents:

UCPRC-TP-2005-01: *HVS Test Plan* (Strategic Plan Element 4.17), March 2005.
UCPRC-RR-2006-10: *Construction and Preliminary HVS Tests of Pre-cast Concrete Pavement Slabs* (Strategic Plan Element 4.17), January 2007.

Signatures:

E. Kohler **1st Author**	W. Nokes **Technical Review**	D. Spinner **Editor**	J. Harvey **Principal Investigator**	M. Samadian **Caltrans Contract Manager**

DISCLAIMER

The contents of this report reflect the views of the authors who are responsible for the facts and accuracy of the data presented herein. The contents do not necessarily reflect the official views or policies of the State of California or the Federal Highway Administration. This report does not constitute a standard, specification, or regulation.

UPDATED VERSION

The original version of this Technical Memorandum (UCPRC-TM-2007-03) was delivered to Caltrans by the University of California Pavement Research Center (UCPRC) on November 1, 2005, within six weeks after completion of the first HVS test. The six-week goal was set by Caltrans. This updated document is a revision of the original, with changes made in December 2006 and June 2007 to correct some HVS wheel load levels, and to include minor editorial and formatting changes that make the document consistent with others prepared by UCPRC.

PROJECT OBJECTIVES

The purpose of this research is to provide data and knowledge to help meet Caltrans' short-term and long-term needs:

- The short-term need is to provide information to District 8 about failure mechanisms and performance of pre-cast concrete using the Super-Slab® panels constructed and tested in District 8. Failure and performance information will be provided so District 8 can decide if performance is comparable or better than currently available rehabilitation strategies.
- The long-term need is to provide test and performance data about this potential alternative to current LLPRS designs. Comparisons with load repetitions and failure mechanisms from HVS field tests on LLPRS designs are expected to provide District 8 with information about relative indicators of pavement performance of Super-Slab (along with other factors, e.g., constructability and costs, which are not addressed in the Test Plan) in their overall assessment of Super-Slab as a potential alternative to LLPRS as well as conventional PCC rehabilitation strategies.

This research project has been designed to provide Caltrans with data and information about Super-Slab so that Caltrans can make decisions about pavement policy, specifications, design, and related issues. The test plan was responsive to the topics identified by District 8 (in their request to Caltrans Pavement Standards Team (PST) for evaluation) by providing the following:

1. Short-term performance of longitudinal joint between Super-Slab® and adjacent lane and shoulder.
    - Longitudinal and transverse joint pavement behavior:
    - Magnitude of load transfer across (i) tied longitudinal joint between adjacent Super-Slab panels and (ii) doweled transverse joints.
    - Observed (if any) visible joint deterioration at all joints including visual inspection and photographs to document separation or other deterioration at the interface between the panels and the AC shoulder.
2. Short-term performance of smoothness including settlement issues, caused by (1) faulting and cracking and (2) settlement that results from slab and CTB deterioration.

3. Long-term performance of Super-Slab®, including life expectancy, utilizing HVS testing.
    - Data on failure mechanisms (e.g., cracking) and number of load repetitions on Super-Slab under HVS loading at one field site.
    - Estimation of expected service life of Super-Slab pavement based on HVS test results.

TABLE OF CONTENTS

List of Figures ..... **vii**
List of Tables ..... **viii**
1. INTRODUCTION **1**
2. HVS TEST 597FD **4**
2.1 Test Section Instrumentation and Test Program 4
2.2 Visual Condition of Section 597FD 7
2.3 MDD Data for Test 597FD 10
2.3.1 Deflections and Load Transfer Efficiency from MDDs 15
2.3.2 Conclusions Drawn from MDD Data 19
2.4 Vertical JDMD Data for Test 597FD 19
2.4.1 Deflections and Load Transfer Efficiency from JDMDs 22
2.4.2 Conclusions Drawn from JDMD Data 24
2.5 Horizontal JDMD data for Test 597FD 24
2.6 Structural Capacity of Section 597FD 28
3. INTERIM CONCLUSIONS **31**
4. REFERENCES **32**

LIST OF FIGURES

Figure 1: Test section layout and HVS during load testing. 4
Figure 2: Thermocouple JDMD and MDD locations for Test 597FD. 5
Figure 3: Pavement cross section and MDD depths. 6
Figure 4: Hairline initial cracks confined to the trafficked area of Section 597FD. 10
Figure 5: Fully developed corner cracks at the transverse joint close to the cabin-end of Section 597FD. 10
Figure 6: Typical MDD data obtained from MDD 1 for Test 597FD. 11
Figure 7: Peak deflection summary for MDD 3 for the duration of Test 597FD. 12
Figure 8: 60 kN peak deflection summary for MDD 3 for the duration of Test 597FD. 13
Figure 9: 60 kN peak deflection for MDD 3 plotted against the temperature gradient in the pre-cast PCC slab for different trafficking loads. 14
Figure 10: 60 kN peak deflection for MDD 3 plotted against the temperature gradient in the pre-cast PCC slab for the 60 kN trafficking load. 14
Figure 11: Formulation of the Load Transfer Efficiency. 16
Figure 12: Initial 60 kN approach and leave slab deflection for the transverse joint between MDDs 3 and 4. 17
Figure 13: Final 60 kN approach and leave slab deflection for the transverse joint between MDDs 3 and 4. 17
Figure 14: 60 kN LTE at the transverse joint between MDDs 1 and 2 for the duration of Test 597FD. 18
Figure 15: 60 kN LTE at the transverse joint between MDDs 3 and 4 for the duration of Test 597FD. 18
Figure 16: Typical JDMD data obtained from JDMDs 1 and 2 for Test 597FD. 20
Figure 17: Typical JDMD data obtained from JDMD 3 for Test 597FD. 20
Figure 18: JDMD deflection and LTE summary for JDMDs 1 and 2 at all deflection load levels for the duration of Test 597FD. 21
Figure 19: JDMD deflection and LTE summary for JDMDs 1 and 2 at the 60 kN deflection load for the duration of Test 597FD. 22
Figure 20: Initial JDMD deflection and LTE data for JDMDs 1 and 2 at the 60 kN deflection load plotted against the slab temperature gradient. 23

Figure 21: Final JDMD deflection and LTE data for JDMDs 1 and 2 at the 60 kN deflection load plotted against the slab temperature gradient. 23
Figure 22: Typical transverse joint activity result from JDMDs 13 and 14. 25
Figure 23: 60 kN joint activity of the cabin-end transverse joint recorded by JDMD 13. 25
Figure 24: 60 kN joint activity of the tow-end transverse joint recorded by JDMD 14. 26
Figure 25: Joint activity of the cabin-end transverse joint recorded by JDMD 13 plotted against the temperature gradient of the slab. 27
Figure 26: Joint activity of the tow-end transverse joint recorded by JDMD 14 plotted against the temperature gradient of the slab. 27
Figure 27: Distribution of ESALS for a condition of corner crack initiation at 50 percent of the transverse joints. 30

LIST OF TABLES

Table 1: SI* (Modern Metric) Conversion Factors ix
Table 2: Test Program for HVS Test 597FD 8
Table 3: Summary of Visual Crack Observations on Section 597FD 9
Table 4: Periods of Valid MDD Data for Test 597FD 11

Table 1: SI* (Modern Metric) Conversion Factors

APPROXIMATE CONVERSIONS TO SI UNITS				
Symbol	**Convert From**	**Multiply By**	**Convert To**	**Symbol**
LENGTH				
in	inches	25.4	millimeters	mm
ft	feet	0.305	meters	m
AREA				
in^2	square inches	645.2	square millimeters	mm^2
ft^2	square feet	0.093	square meters	m2
VOLUME				
ft^3	cubic feet	0.028	cubic meters	m^3
MASS				
lb	pounds	0.454	kilograms	kg
TEMPERATURE (exact degrees)				
°F	Fahrenheit	5 (F-32)/9 or (F-32)/1.8	Celsius	C
FORCE and PRESSURE or STRESS				
lbf	poundforce	4.45	newtons	N
lbf/in^2	poundforce/square inch	6.89	kilopascals	kPa
APPROXIMATE CONVERSIONS FROM SI UNITS				
Symbol	**Convert From**	**Multiply By**	**Convert To**	**Symbol**
LENGTH				
mm	millimeters	0.039	inches	in
m	meters	3.28	feet	ft
AREA				
mm^2	square millimeters	0.0016	square inches	in^2
m^2	square meters	10.764	square feet	ft^2
VOLUME				
m^3	cubic meters	35.314	cubic feet	ft^3
MASS				
kg	kilograms	2.202	pounds	lb
TEMPERATURE (exact degrees)				
C	Celsius	1.8C+32	Fahrenheit	F
FORCE and PRESSURE or STRESS				
N	newtons	0.225	poundforce	lbf
kPa	kilopascals	0.145	poundforce/square inch	lbf/in^2

*SI is the symbol for the International System of Units. Appropriate rounding should be made to comply with Section 4 of ASTM E380. (Revised March 2003)

1. INTRODUCTION

Caltrans District 8 is in the process of evaluating the use of pre-cast PCC panels as an alternative long-life pavement rehabilitation strategy. One such option is the Super-Slab® System (Super-Slab®), developed in 2000 by The Fort Miller Co., Inc., of Schuylerville, New York. The Long-Life Pavement Rehabilitation Strategy (LLPRS) of the California Department of Transportation (Caltrans) and the role of the evaluation by District 8 in this strategy are outlined in the HVS test plan previously prepared by the Partnered Pavement Research Program (1).

The District's draft Evaluation Plan identified four objectives in their pilot program. The first three objectives focus on evaluation of a trial project, while the fourth objective includes evaluation of the long-term performance of Super-Slab, including life expectancy, utilizing the HVS. [1]

1. Short-term performance of longitudinal joint between Super-Slab® and adjacent lane and shoulder.
    - Longitudinal and transverse joint pavement behavior:
    - Magnitude of load transfer across (i) tied longitudinal joint between adjacent Super-Slab panels and (ii) doweled transverse joints.
    - Observed (if any) visible joint deterioration at all joints including visual inspection and photographs to document separation or other deterioration at the interface between the panels and the AC shoulder.
2. Short-term performance of smoothness including settlement issues, caused by (1) faulting and cracking and (2) settlement that results from slab and CTB deterioration.
3. Long-term performance of Super-Slab, including life expectancy, utilizing HVS testing.
    - Data on failure mechanisms (e.g., cracking) and number of load repetitions on Super-Slab under HVS loading at one field site.
    - Estimation of expected service life of Super-Slab pavement based on HVS test results.

[1] Bullet points were not in the original District 8 draft Evaluation Plan, but were added by UCPRC to expand and support corresponding topic headings.

The information contained in this memo only covers the data from the first loading Test 597FD (Dry).

Test 597FD was the first HVS test done at the San Bernardino test site, where pre-cast concrete panels were constructed at the Cherry Avenue off-ramp near the interchange of highways I-15 and SR 210 in San Bernardino County. It was preceded by a series of thermal curl tests and HVS load tests on the ungrouted pre-cast slabs.

This technical memorandum, one of a series of reports on HVS testing, originally aimed to give Caltrans an early indication of the expected behavior and performance based on accelerated loading with the HVS. A draft memorandum was given to Caltrans in November 2005, six weeks after the first HVS test (597FD) was completed. This schedule for reporting results was set by Caltrans to enable District 8 to make an informed decision about including the pre-cast PCC pavement in the bidding process for projects then slated on I-15 near the I-15/SR210 interchange.

The results from the earlier thermal curling tests and ungrouted load tests appear in a separate report that also includes construction details, such as site preparation, slab placement, and material characterization (2).

It has to be emphasized that the results and conclusions presented in this memorandum are subject to the very specific set of conditions under which the HVS tests were performed. Given the normal variable nature of pavement support and environmental conditions, the results and conclusions are not applicable in general but they do provide a useful first indication of what behavior and performance may be expected from the pre-cast PCC pavement in other projects. Specific items that should be noted include:

- *The pavement support conditions at the San Bernardino test site.* The cement-treated base (CTB) was specifically constructed for the HVS tests, and it was new and undamaged at the time of the tests. It is expected that the base layers of

existing pavements to undergo rehabilitation will have deteriorated and therefore provide substantially less support to the pre-cast PCC pavement.

- *The environmental conditions during the HVS test.* Test 597FD was done during the summer of 2005 with no substantial rainfall occurring and no water being applied to the test section during the test. The test was therefore done under optimal environmental conditions with the dry subgrade providing good support and no erosion and pumping from the PCC/CTB interface.
- *The construction process.* Normal construction would usually happen under more routine circumstances. For example, it is expected that the pre-cast PCC pavement will be placed almost exclusively during nighttime closures with limited time being available. This did not apply to the construction of the test site at San Bernardino. Although it may be argued that the construction crew was inexperienced, great care was exercised by the crew under the direction of the vendor during the construction process to provide good construction quality, and construction was done during daytime with little time restraint.

2. HVS TEST 597FD

2.1 Test Section Instrumentation and Test Program

This section provides an overview of the instrumentation of Section 597FD, the loading sequence applied to the section, and the schedule for data collection. Ten slabs were manufactured and placed in a 5x2 pattern. The load occurred as shown in Figure 1. The instrumentation for Section 597FD was concentrated mostly on the center slab in the north side of the 5x2 grid, as shown in Figure 2. The area of the slabs not exposed to direct sunlight, due to the HVS and its shade, is indicated in the figure as well.

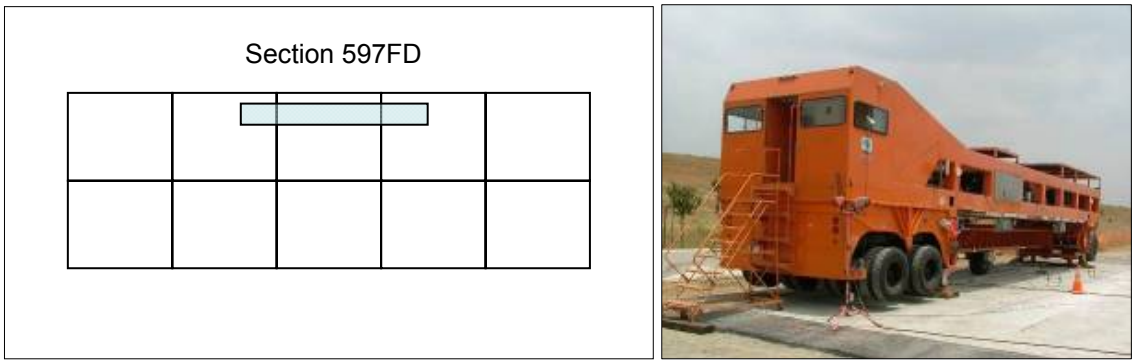

Figure 1: Test section layout and HVS during load testing.

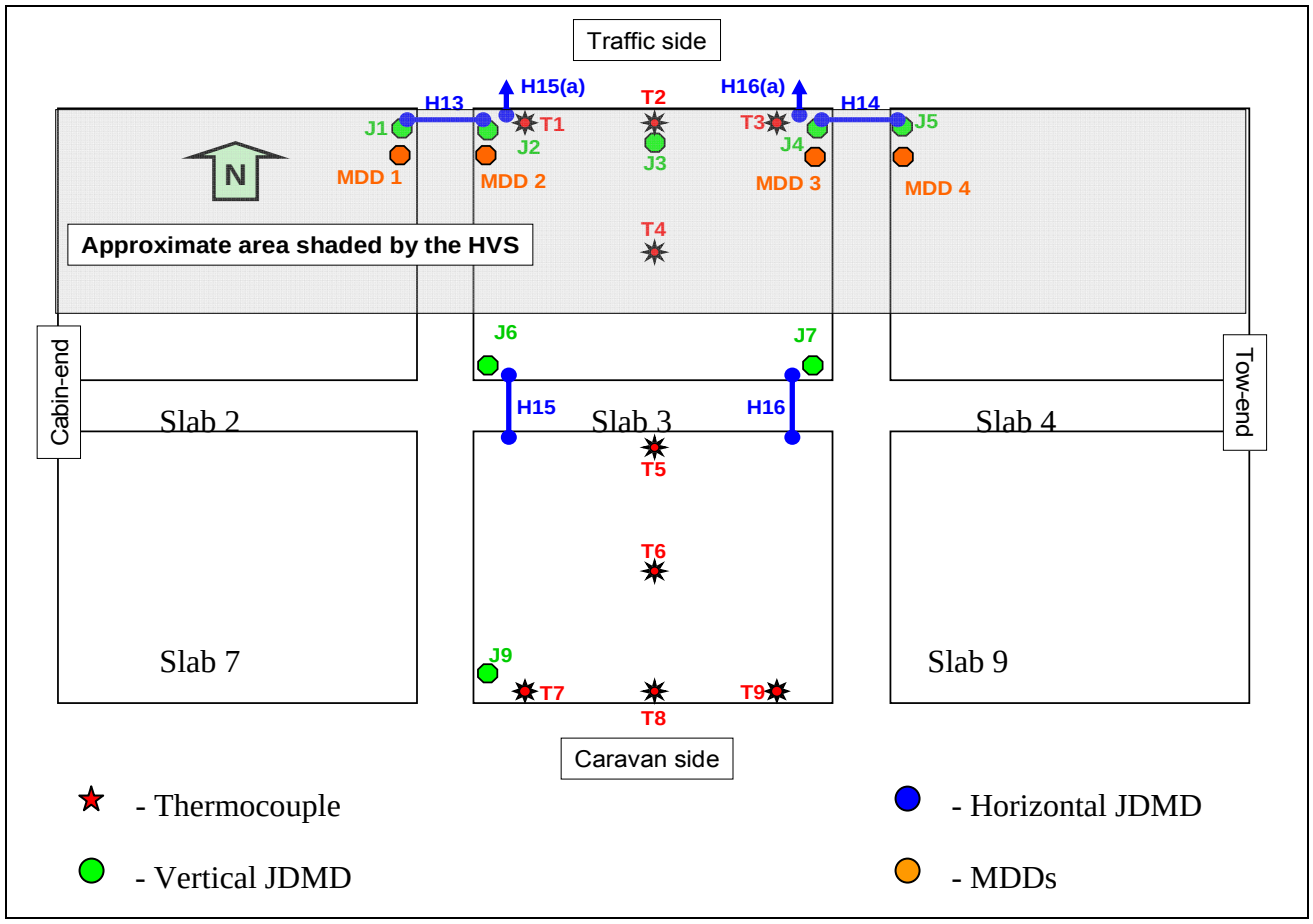

Figure 2: Thermocouple JDMD and MDD locations for Test 597FD.

The slabs are 4.572 m long by 3.962 m wide (15 by 13 ft)[2], 220 mm thick (8½ in), and are joined with dowels and tie bars. The exact details of the construction of the slabs and the instrumentation used are detailed in the construction report (2). The symbol "J" is used to indicate vertical joint deflection measurement devices (JDMDs). The symbol "H" is used to indicate horizontal JDMDs in Figure 2. Thermocouples were installed at depths of 10, 60, 110, 160 and 210 mm (0.4, 2.4, 4.3, and 8.3 in) in the 220-mm thick slabs. In addition to the joint sensors (JDMDs), Multi-depth Deflectometer stacks (MDDs) were installed in close proximity to vertical JDMDs 1, 2, 4, and 5 for Test 597FD. The MDD modules were installed in the top-cap as close to the surface as possible, at 230 mm (9 in) depth at the top of the CTB, at 380 mm (15 in) depth at the bottom of the CTB and at 680 mm (27 in) depth in the subgrade. All MDDs

[2] Units in the US customary system are included in parenthesis in this section of the document, in addition to the SI units. Dual units are not used in the rest of the document.

and vertical JDMDs were anchored at a depth of 3 m (10 ft). Figure 3 shows the pavement cross section and the location of the MDDs through the pavement structure.

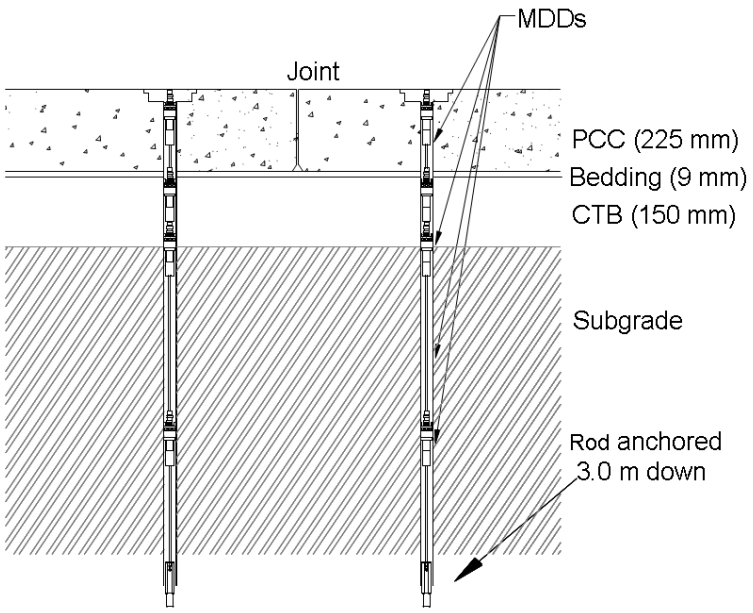

Figure 3: Pavement cross section and MDD depths.

The initial test program for HVS Test 597FD is shown in Table 2. A distinction is made between the trafficking load and the deflection load. The trafficking load is the wheel-load at which the load repetitions are applied to the test section and the deflection load is the load at which deflections are recorded throughout the test. The trafficking load is the load that causes the damage to the pavement during the test. As an example, the trafficking load for the most part of Test 597FD was a 150 kN (34 kips), single aircraft tire load inflated to 1,440 kPa (209 psi) inflation pressure. However, deflections were collected at three hourly intervals under the 150 kN (34 kips) load and at regular intervals under deflection loads of 60, 80, and 120 kN (14, 18, 27 kips). Trafficking was done in the bidirectional mode. The test program in Table 2 only provides an indication of when the traffic load was increased and when deflections were recorded. The actual repetitions at which these activities occurred may differ slightly from the test program.

In addition to the deflection data obtained from the MDDs and JDMDs and the temperature data obtained from the thermocouples, visual condition information was collected in the format of digital still images. The data obtained from each of these processes are presented in Section 2.2 through Section 2.6 of this report. An example of a typical individual data reading is presented first and it is followed by a summary of the particular type of data for the duration of

the test with a description of the general trends observed in the summary data. In the case of the MDD and JDMD data, the Load Transfer Efficiency (LTE) was calculated at each of the transverse joints and the LTE is summarized for the duration of Test 597FD.

2.2 Visual Condition of Section 597FD

The visual condition of the test section was observed for the duration of the test, primarily to determine whether any cracks developed. Visible cracks appeared on the surface of the test section at the number of load repetitions summarized in Table 3.

Table 2: Test Program for HVS Test 597FD

HVS Test Sheet:	597FD	**Pavement:**	220 mm PCC/9 mm bedding/150 mm CTB	**Version:**	Final
Location:	Cherry Ave offramp, I15 & SR210	**Test Start Date:**	08-Jun-05		
Wheel configuration:	Aircraft single wheel	**Instrumentation**	*Thermocouple*	TC1 to TC9 (All depths)	
Traffic:	Bi-directional		*JDM*	JDMD1, JDMD2, JDMD3, JDMD4, JDMD5, C1, C2	
Wander:	None			H13, H14, H16, H15(a), H16(a)	
Temperature Condition:	Uncontrolled		*MD*	MDD1, MDD2, MDD3 and MDD4	
				MDD levels: Top-cap, 230mm, 280mm and 680mm deep	
Authorizing Signature:	**Hechter Theyse, May 2006**		*Strain Gauge (SG)*	None	

						Deflection loads (kN)					
Repetition / Time	**Traffic load (kN, kPa)**	**Water added**	**Control Box Temp**	**Profilometer**	**TCs**	**JDMD**	**MDD**	**SG**	**Crack detection and marking**	**Digital Photographs**	**Comments**
10	60, 1440	No	Off	-	Yes	60	60	-	yes	yes	Start at 60kN
50 000	60, 1440	No	Off	-	Yes	60	60	-	yes	-	
100 000	60, 1440	No	Off	-	Yes	60	60	-	yes	yes	
150 000	80, 1440	No	Off	-	Yes	60, 80	60, 80	-	yes	-	Increase to 80kN
200 000	80, 1440	No	Off	-	Yes	60, 80	60, 80	-	yes	yes	
250 000	80, 1440	No	Off	-	Yes	60, 80	60, 80	-	yes	-	
300 000	120, 1440	No	Off	-	Yes	60, 80, 120	60, 80, 120	-	yes	yes	Increase to 120kN
350 000	120, 1440	No	Off	-	Yes	60, 80, 120	60, 80, 120	-	yes	-	
400 000	120, 1440	No	Off	-	Yes	60, 80, 120	60, 80, 120	-	yes	-	
150 000	120, 1440	No	Off	-	Yes	60, 80, 120	60, 80, 120	-	yes	-	
500 000	150, 1440	No	Off	-	Yes	60, 80, 120, 150	60, 80, 120	-	yes	-	
550 000	150, 1440	No	Off		Yes	60, 80, 120, 150	60, 80, 120,150	-	yes	yes	Increase to 150kN
600 000	150, 1440	No	Off	-	Yes	60, 80, 120,150	60, 80, 120,150	-	yes	yes	

If no failure is detected after 600 000 reps, continue with measurements at 50 000 repetition increments until failure

The above deflection reading are taken on demand at the indicated number of repetitions, in addition to these readings, deflection also needs to be recorded on the fly at 3 hour intervals at 9h00, 12h00, 15h00, 18h00, 21h00, 00h00, 3h00 and 06h00

General Notes

a. A set of overlapping photographs that spans the full length of the test section has to be taken at the indicated times
b. Photographs to be taken whenever cracks appear or crack growth is detected

Specific notes

a.

Table 3: Summary of Visual Crack Observations on Section 597FD

Load Repetitions	Crack Description	Instruments in Close Proximity
54,815	Hairline cracks confined to the trafficked area.	-
762,044	Corner cracks at the transverse joint on the cabin-end of the test section (Figure **2**). The crack on the MDD1/JDMD1 side of the transverse joint only extended from the transverse joint to about halfway into the trafficked area. The crack on the MDD2/JDMD2 side of the transverse joint was fully developed and extended form the transverse joint to the shoulder joint.	MDD 1 and 2 JDMD 1 and 2 Horizontal JDMDs 13 and 15(a)
844,648	Corner cracks at the transverse joint on the cabin-end of the test section (Figure **2**). Cracks on either side of the transverse joint fully developed and extending from the transverse joint to the shoulder joint.	MDD 1 and 2 JDMD 1 and 2 Horizontal JDMDs 13 and 15(a)

Initially, only hairline cracks appeared in the trafficked area of the test section. These cracks may have been caused by the high contact stresses under the single aircraft tire as it was inflated to a pressure of 1,440 kPa or, more likely, the cracks are shrinkage cracks caused during the curing of the slabs that became exposed by the abrasive action of the trafficking loads. The main structural corner cracks were first observed at 762,044 repetitions and were fully developed at 844,648 load repetitions. The corner cracks did, however, only develop at the transverse joint closest to the cabin-end of the test section during Test 597FD. The influence of the corner cracks on the deflection response of the pre-cast pavement is investigated in Section 2.6. Figure 4 shows a photograph of the initial hairline cracks and Figure 5 shows photographs of the fully developed corner cracks.

Figure 4: Hairline initial cracks confined to the trafficked area of Section 597FD.

(a) Corner crack on JDMD1 side of the cabin-end transverse joint

(b) Corner crack on JDMD2 side of the cabin-end transverse joint

Figure 5: Fully developed corner cracks at the transverse joint close to the cabin-end of Section 597FD.

2.3 MDD Data for Test 597FD

MDD data were collected according to the schedule shown in Table 2. The number of MDD channels available on the data acquisition system limited the number of MDD modules that could be installed to those shown in Figure 2. The in situ material at the test site seemed to consist mostly of sandy material containing many large stones (2), which caused problems during the installation of the MDDs by making it difficult to drill the holes for the MDDs and to properly fix their modules at the predetermined depths. At times, data from certain of the MDD modules were therefore questionable, and these data were removed from the data set and not incorporated in any analysis. Table 4 provides a

summary of the periods of testing during which valid data were obtained from each of the MDDs.

Table 4: Periods of Valid MDD Data for Test 597FD

MDD	Sensor Depths [mm]	Period of Valid Data [repetitions]
1	0, 230, 380, 680	0 to 527,465
2	0, 230	0 to 527,465
3	0, 230, 380	0 to 922,246 1,025,012 to 1,239,262
4	0, 230, 380	0 to 922,246 1,025,012 to 1,239,2262

An example of the depth deflection bowls obtained from the MDD system is shown in Figure 6 for the 74th, 76th and 78th load repetitions which were recorded with the wheel running in the same direction under a 60kN load. Except for the MDD module at a depth of 380 mm, there is very little noise in the data and the deflection results of the three load cycles are highly repeatable. Similar results were also obtained for the other MDD stacks. The peak deflections were extracted from the depth deflection bowls and the peak deflection from the surface deflection bowl was used in the subsequent analysis of the LTE.

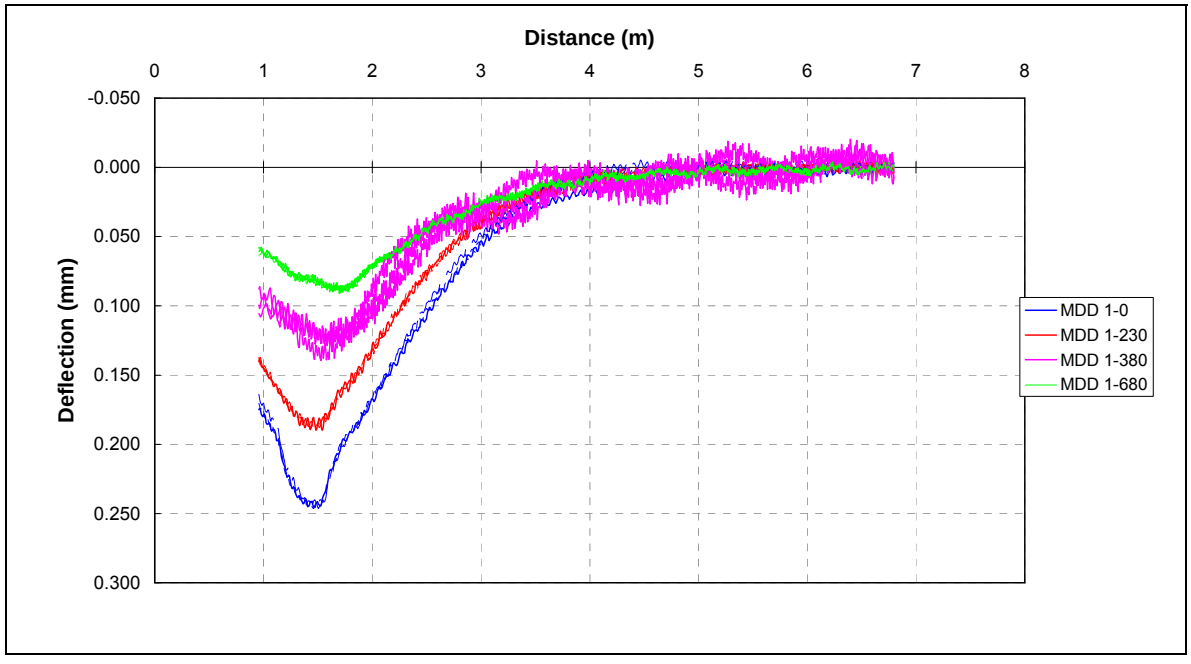

Figure 6: Typical MDD data obtained from MDD 1 for Test 597FD.

Figure 7 shows a summary of the peak deflections for MDD 3 for the duration of Test 597FD. The peak deflections are shown for all the deflection loads from 60 to 150 kN and the trafficking load is shown at the top of the chart. The variability in Figure 7 for each sensor indicates the presence of daily cycles, with three factors affecting the peak deflection: These are:

- The magnitude of the deflection load, with a higher deflection load causing a higher deflection;
- Temperature changes causing a daily change in the peak deflections; and
- Increased depth reduces the daily temperature effects.

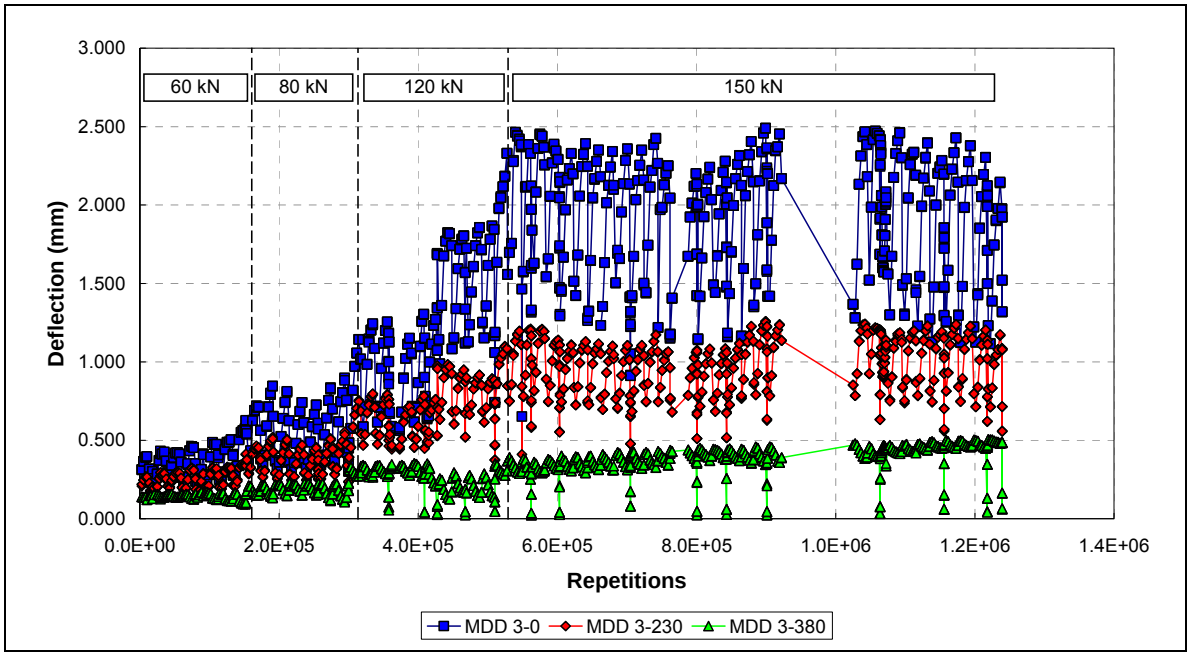

Figure 7: Peak deflection summary for MDD 3 for the duration of Test 597FD.

The first step in eliminating the effect of the deflection load on the data shown in Figure 7 is to extract only the deflections recorded at a 60 kN deflection load from the data set. Figure 8 shows only the 60 kN deflections for the duration of Test 597FD. The effects of daily temperature changes and damage on the deflection are apparent from Figure 8, with the 60 kN deflection showing a general increasing trend with increasing number of load repetitions because of increasing damage inflicted on the pavement.

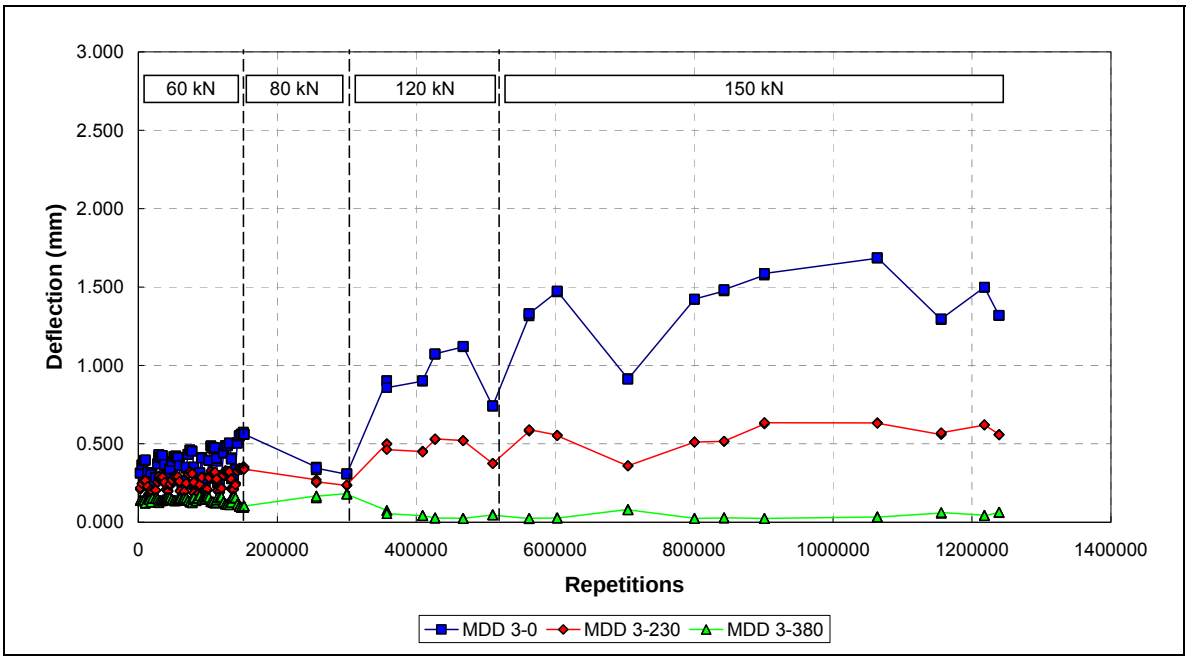

Figure 8: 60 kN peak deflection summary for MDD 3 for the duration of Test 597FD.

The temperature data recorded at depths of 10 mm and 210 mm at thermocouple T1 for the duration of Test 597FD were used to calculate the temperature gradient throughout the slab in an attempt to isolate the effect of daily temperature changes from the 60 kN deflection response of the pavement. The results from this process are shown in Figure 9 for the 60, 80, 120, and 150 kN trafficking loads. It is clear that the magnitude of the trafficking load has an effect on the deflection recorded at a 60 kN deflection load, and the 60 kN deflections recorded during the 150 kN trafficking portion of the test is much higher than those recorded during the 60 kN trafficking portion of the test (note the increasing trend of MDD 3 Level 0 in Figure 8). This is a result of the increasing amount of damage caused by the higher trafficking loads. The data from the initial 60 kN trafficking portion of the test were extracted and plotted in Figure 10 to investigate the effect of the temperature gradient on the 60 kN deflection.

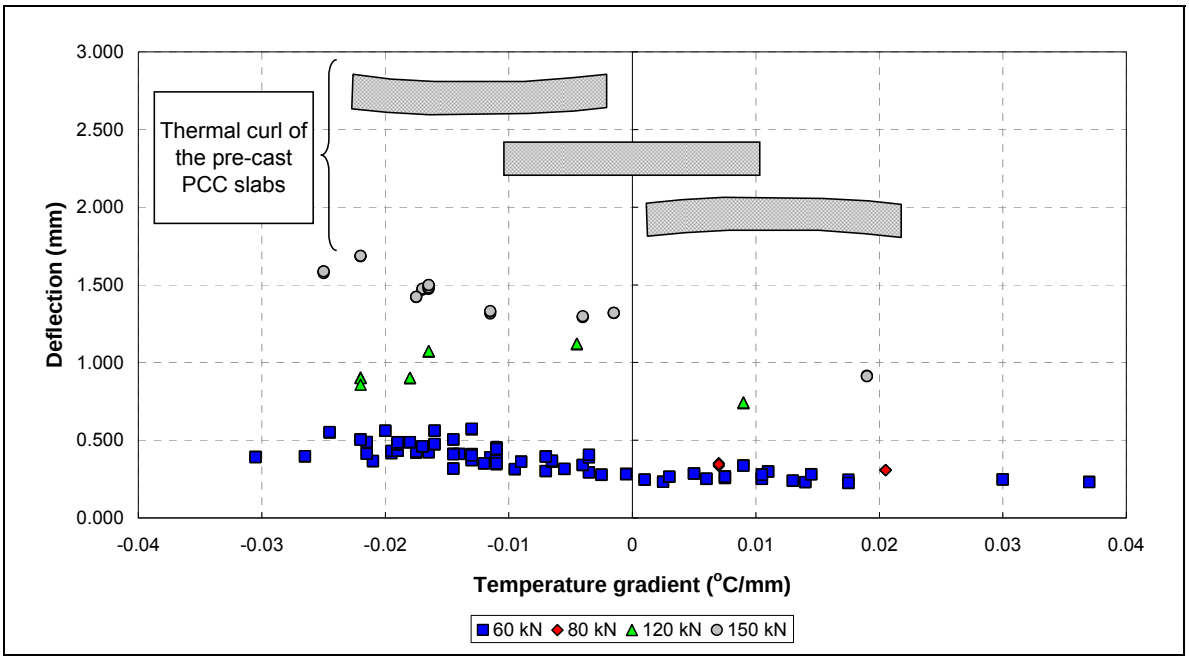

Figure 9: 60 kN peak deflection for MDD 3 plotted against the temperature gradient in the pre-cast PCC slab for different trafficking loads.

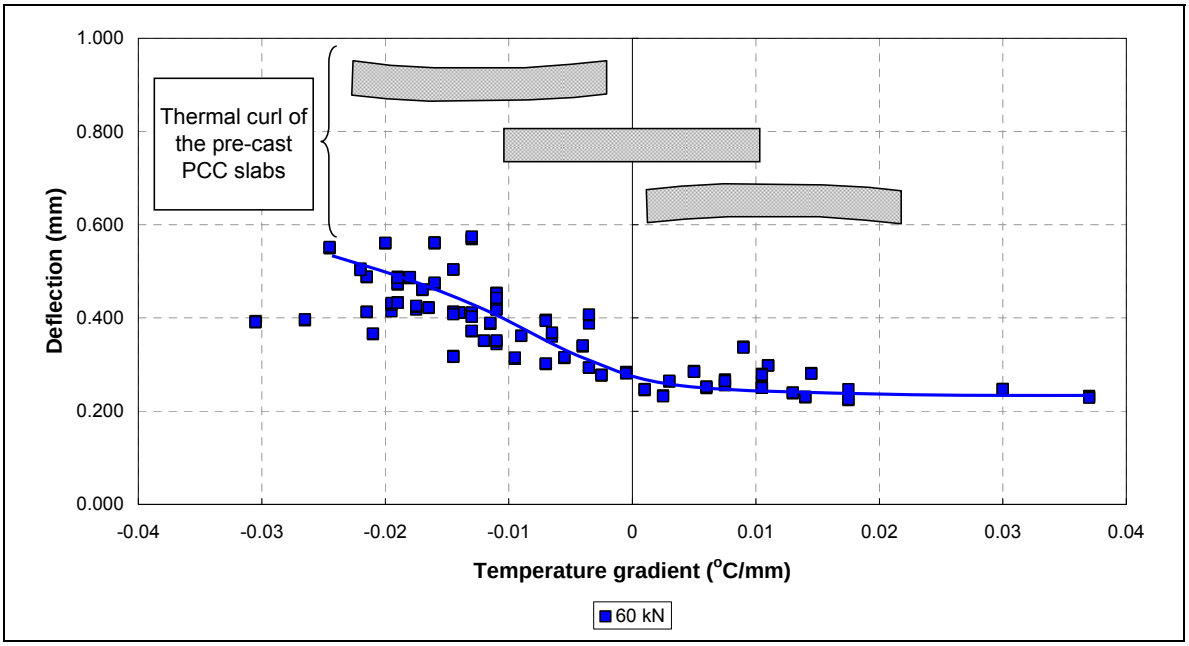

Figure 10: 60 kN peak deflection for MDD 3 plotted against the temperature gradient in the pre-cast PCC slab for the 60 kN trafficking load.

The assumed approximate geometry of the pre-cast PCC slabs is shown at the top of Figure 9 and Figure 10. The slab lay flat when the temperature differential (top to bottom) is equal to that at the time of concrete setting. Since the slabs were not cured on

site but at a local pre-casting plant, it can be assumed that there was no temperature differential at time of setting. If the slab is colder at the surface than at the bottom, a negative temperature gradient is calculated and the corner and edges of the slab curl upwards and could separate from the CTB. If the slab becomes warmer at the top a positive temperature gradient is calculated and the edges of the slab curl downward and rest on the CTB. The deflections at a temperature gradient equal to and higher than zero therefore represents the condition of the slab's edges in contact with the underlayer. As is shown by the trend-line drawn to the data in Figure 10, deflections at MDD3 remain relatively constant at positive temperature gradients. At negative gradients, the thermal curl of the slab causes the edge of the slab to curl upwards, resulting in a longer cantilever effect and higher deflections recorded at the edge of the slab, as is shown by the data on the left-hand side of the chart in Figure 10.

2.3.1 Deflections and Load Transfer Efficiency from MDDs

The process of extracting only the 60 kN deflections and plotting the deflection against the temperature gradient is repeated for the analysis of the LTE in the subsequent paragraphs.

The formulation of the LTE is shown in Figure 11 and is the ratio of the deflection on the leave slab at the time of the peak deflection on the approach slab to the peak deflection on the leave slab. This formulation is based on the assumption that the amount of deflection transferred from the approach to the leave slab when the approach slab is loaded, is proportional to the amount of load transferred from the approach to the leave slab.

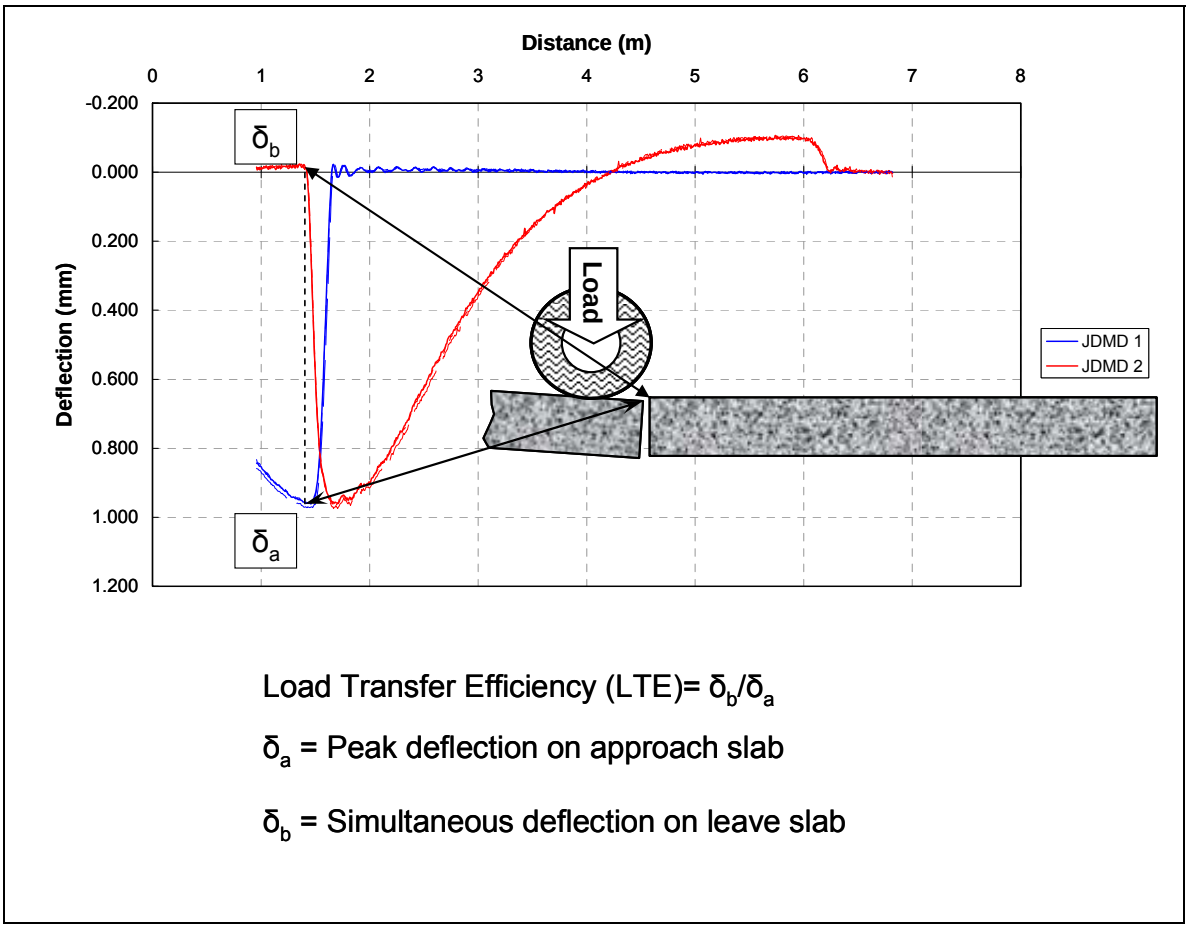

Figure 11: Formulation of the Load Transfer Efficiency.

Figure 12 and Figure 13 show the initial and final 60 kN approach and leave slab deflection used in the calculation of the LTE (initial refers to the beginning of accelerated loading, and final refers to responses after 1.24 million repetitions). The effect of the change in structural condition caused by the HVS trafficking is again apparent when the results from these two figures are compared. Figure 14 and Figure 15 show the LTE calculated for the doweled transverse joints at MDDs 1 and 2 and MDD 3 and 4 respectively for the duration of Test 597FD.

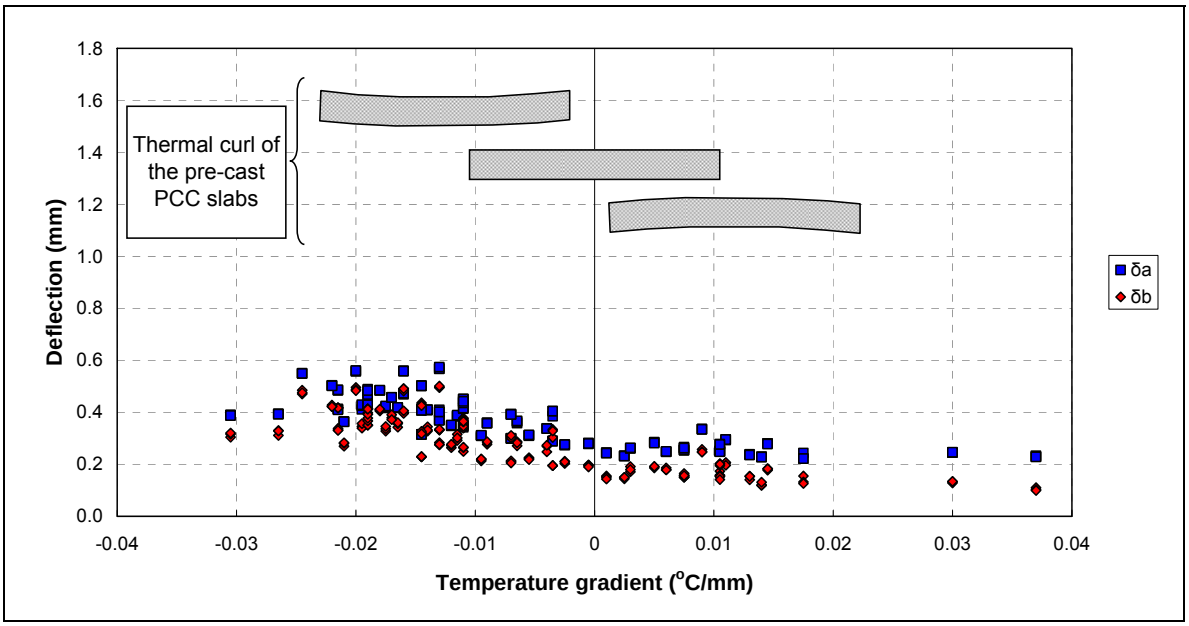

Figure 12: Initial 60 kN approach and leave slab deflection for the transverse joint between MDDs 3 and 4.

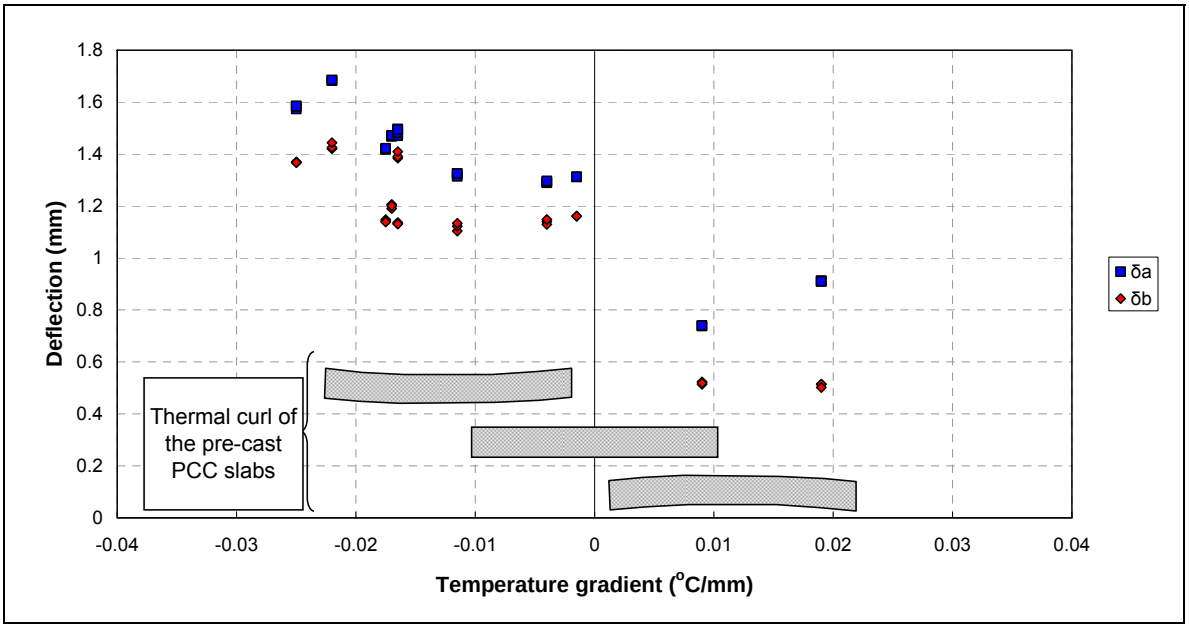

Figure 13: Final 60 kN approach and leave slab deflection for the transverse joint between MDDs 3 and 4.

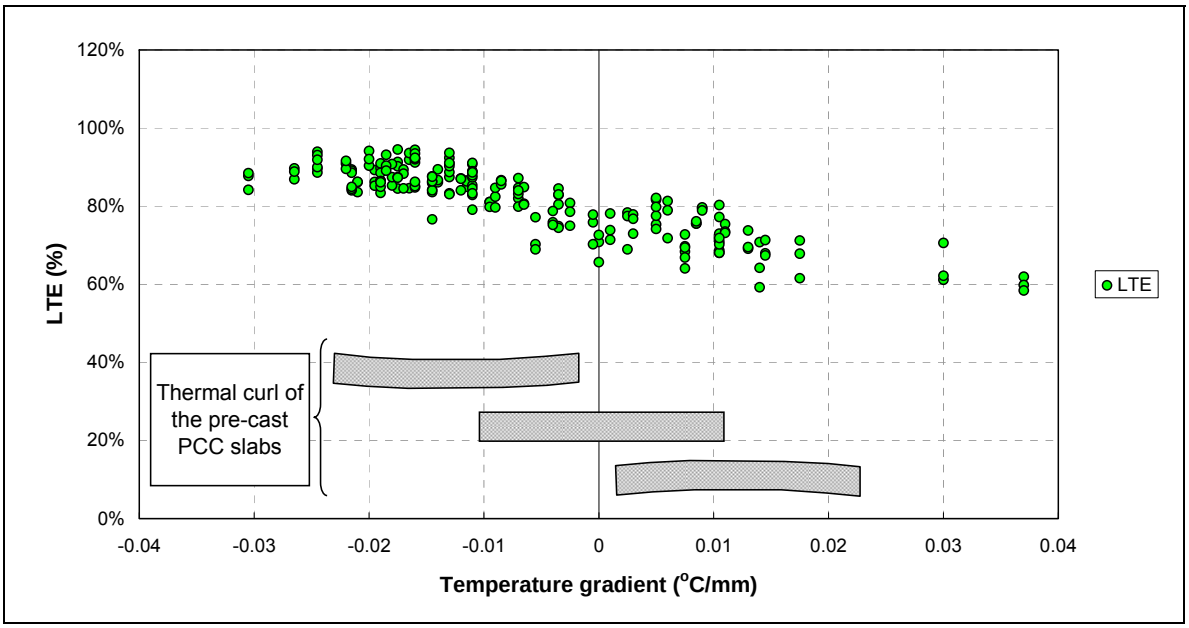

Figure 14: 60 kN LTE at the transverse joint between MDDs 1 and 2 for the duration of Test 597FD.

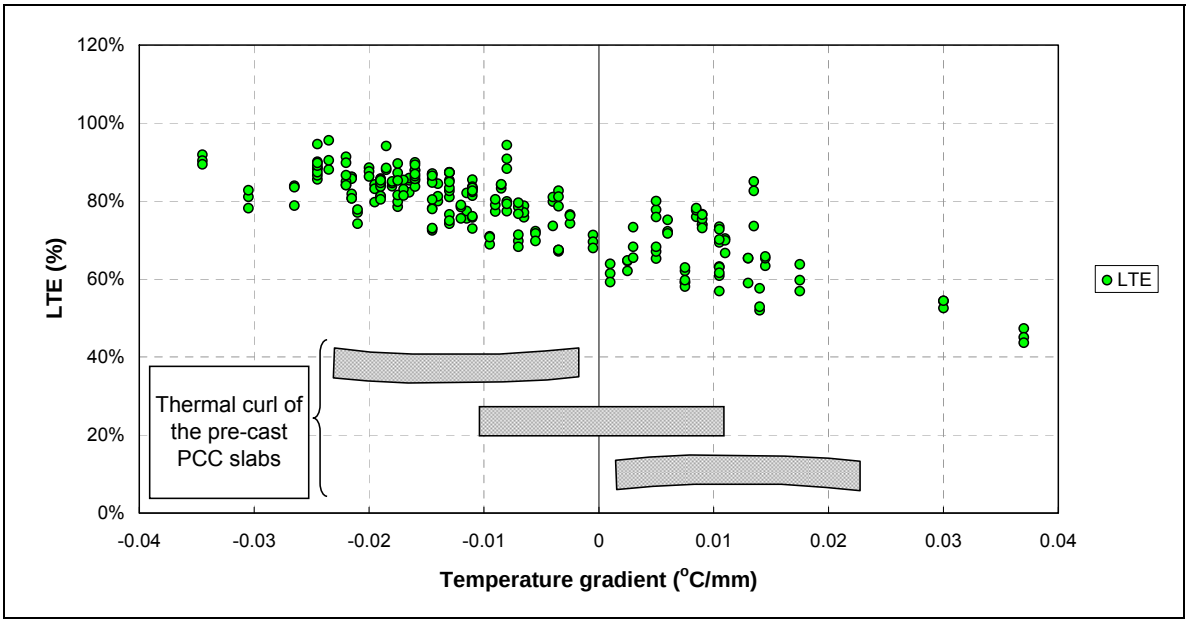

Figure 15: 60 kN LTE at the transverse joint between MDDs 3 and 4 for the duration of Test 597FD.

Although the peak 60 kN MDD deflection plotted in Figure 9, Figure 10, Figure 12, and Figure 13 show an increase in deflection as the test progressed and with decreasing temperature gradient, the LTE does not show any deterioration during Test 597FD. In

terms of LTE there was no damage caused by the HVS test. The LTE does, however, show a decreasing trend with increasing temperature gradient.

2.3.2 Conclusions Drawn from MDD Data

The following conclusions are drawn from the MDD deflection data:

- The magnitude of the MDD deflection depends on the magnitude of the deflection load, with a higher load causing a higher deflection.
- Daily temperature changes in the pre-cast PCC slab cause a temperature gradient in the slab that affects the peak MDD deflection, with the peak MDD deflection increasing at negative temperature gradients.
- The peak MDD deflection from MDD 3 shows that the test section suffered some structural damage during the HVS test, with the MDD deflection increasing from about 0.5 mm to 1.5 mm at a temperature gradient of -0.02°C/mm and increasing from about 0.25 to 1 mm at a temperature gradient of +0.02°C/mm.
- The LTE did not show any deterioration for the duration of Test 597FD (values did not drop significantly) but seems to be affected by the temperature gradient, with the LTE falling from values between 80 and 100 percent at negative temperature gradients to values between 40 and 60 percent at the extreme of the positive temperature gradient range.

2.4 Vertical JDMD Data for Test 597FD

JDMD data were collected according to the schedule shown in Table 2 at the vertical JDMD locations shown in Figure 2. The JDMD instruments are robust and data were obtained from the JDMDs for the full duration of Test 597FD. An example of typical JDMD deflection bowls from the corners of the slabs at the cabin-end transverse joint of Section 597FD is shown in Figure 16 for JDMDs 1 and 2 for the 74th, 76th, and 78th load repetitions. Similar results were also obtained for the other two JDMDs at the tow-end transverse joint on Section 597FD. The peak deflections on the approach slabs and the

simultaneous deflection on the leave slabs were extracted from the JDMD deflection bowls to calculate the LTE based on JDMD data.

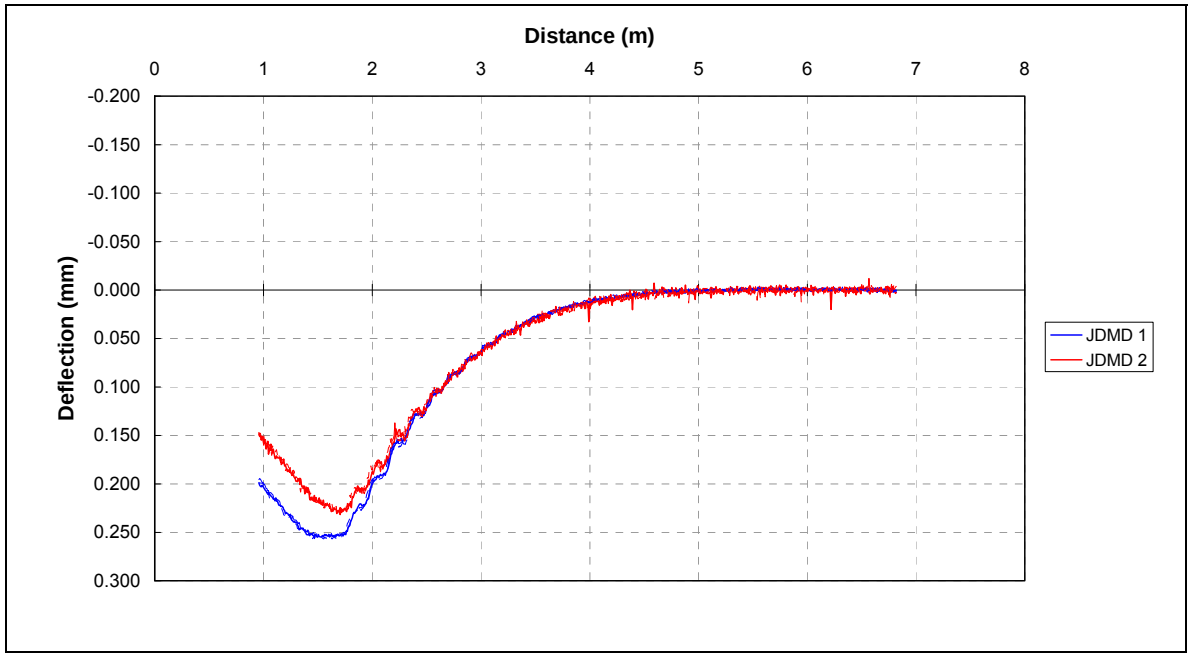

Figure 16: Typical JDMD data obtained from JDMDs 1 and 2 for Test 597FD.

The vertical mid-slab deflection was recorded by JDMD 3, and a typical example of the mid-slab deflection bowl is shown in Figure 17.

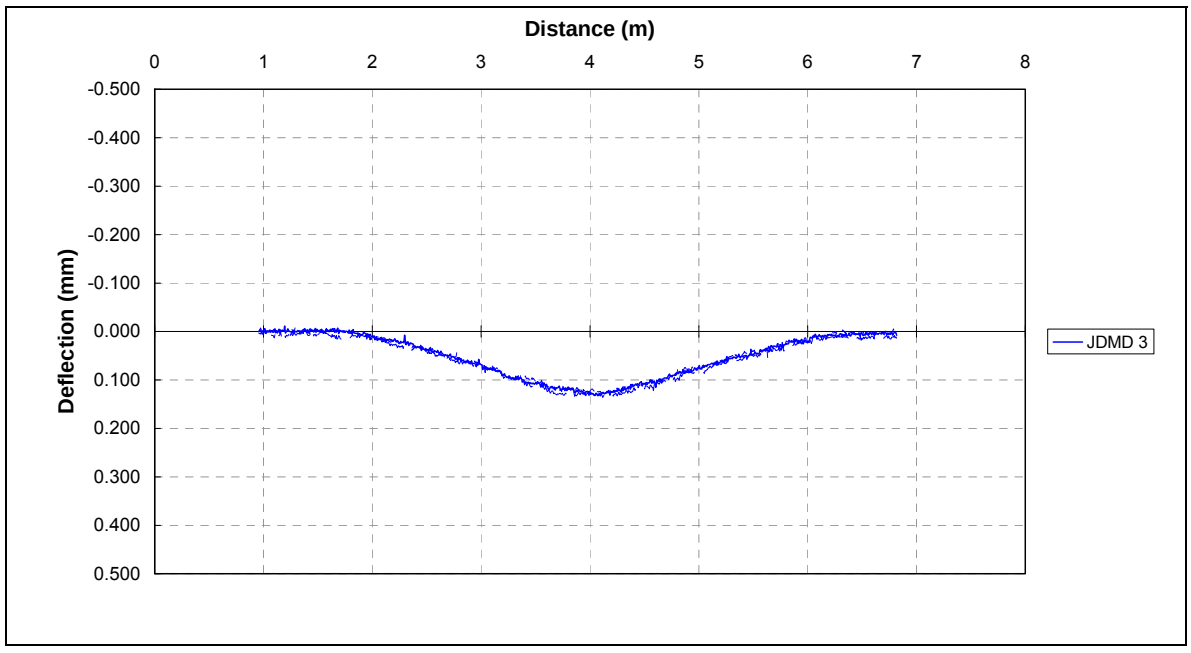

Figure 17: Typical JDMD data obtained from JDMD 3 for Test 597FD.

Figure 18 shows a summary of the peak approach slab deflection, simultaneous leave slab deflection, and LTE from JDMDs 1 and 2 for the duration of Test 597FD for all deflection load levels (the traffic load levels are indicated at the top of the chart). As was the case with the MDD data, the JDMD data clearly exhibits a daily cycle, as shown by scatter around the trend, and there are three factors possibly affecting the deflection and LTE shown in Figure 18. These are:

- The magnitude of the deflection load, with a higher deflection load causing a higher deflection;
- The daily temperature changes causing a daily change in the peak deflections; and
- The amount of damage caused to the pavement, which depends on the magnitude of the trafficking wheel-load and the number of repetitions applied at each particular trafficking load level.

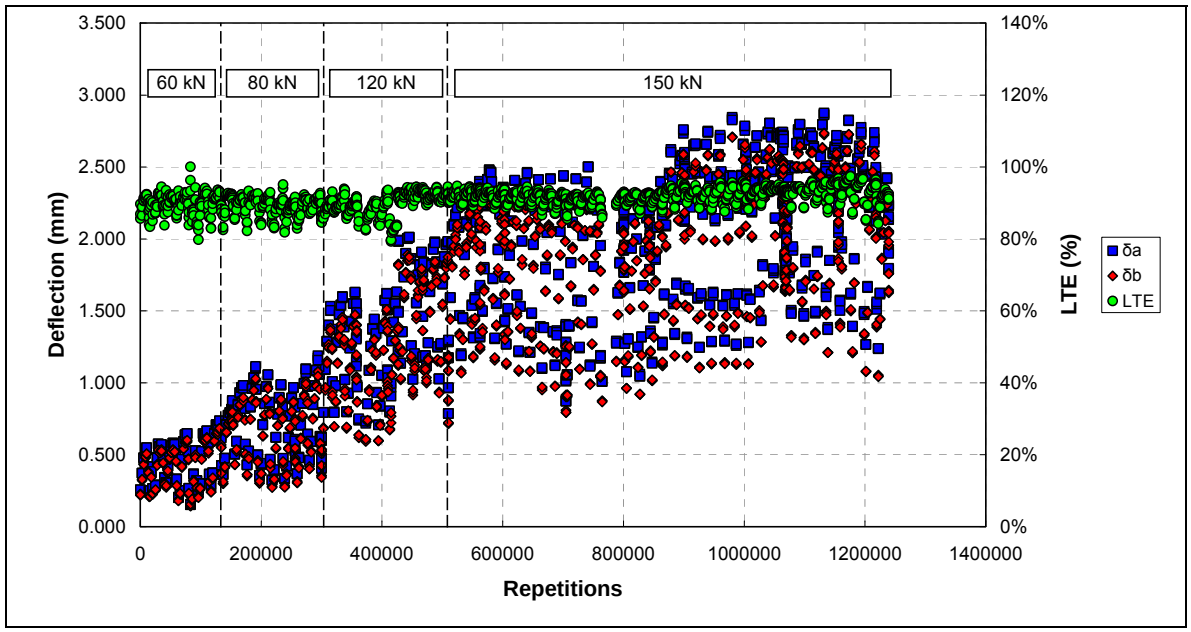

Figure 18: JDMD deflection and LTE summary for JDMDs 1 and 2 at all deflection load levels for the duration of Test 597FD.

2.4.1 Deflections and Load Transfer Efficiency from JDMDs

The JDMD data was therefore processed in the same way as the MDD data by first extracting only the 60 kN data to eliminate the effect of the deflection load. The JDMD deflection and LTE data for JDMDs 1 and 2 at the 60 kN deflection load are shown in Figure 19 for the duration of Test 597FD. Similar results were obtained from JDMDs 3 and 4 at the tow-end transverse joint of Section 597FD.

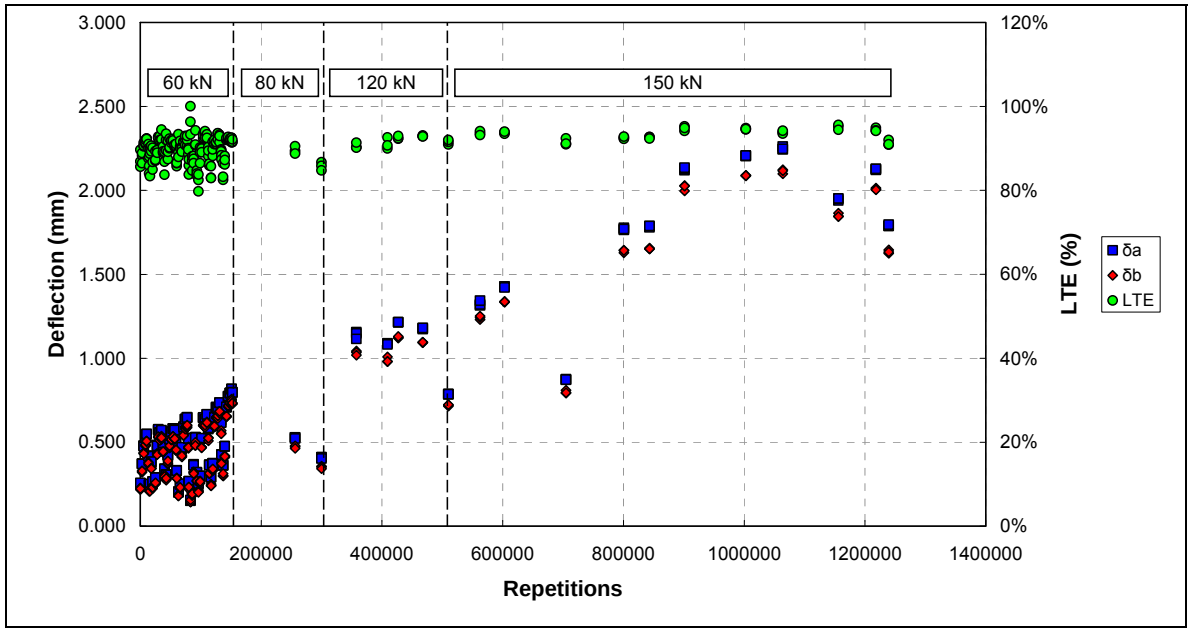

Figure 19: JDMD deflection and LTE summary for JDMDs 1 and 2 at the 60 kN deflection load for the duration of Test 597FD.

The 60 kN deflection data still exhibits an increase in deflection with increasing load repetitions (increasing damage) and a temperature-associated daily cyclic change. The 60 kN JDMD deflection and LTE were therefore plotted against the temperature gradient of the slab as it was with the MDD data. The initial deflection and LTE results for less than 100,000 load repetitions are shown in Figure 20, and the final deflection and LTE results from the 150 kN trafficking portion of the test are shown in Figure 21.

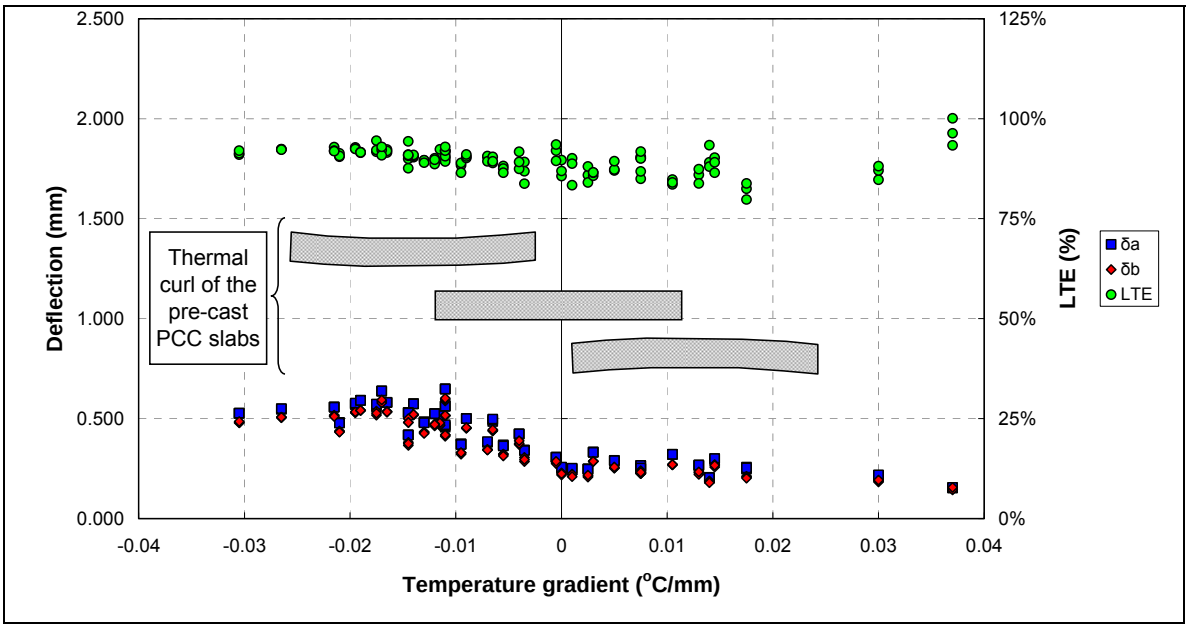

Figure 20: Initial JDMD deflection and LTE data for JDMDs 1 and 2 at the 60 kN deflection load plotted against the slab temperature gradient.

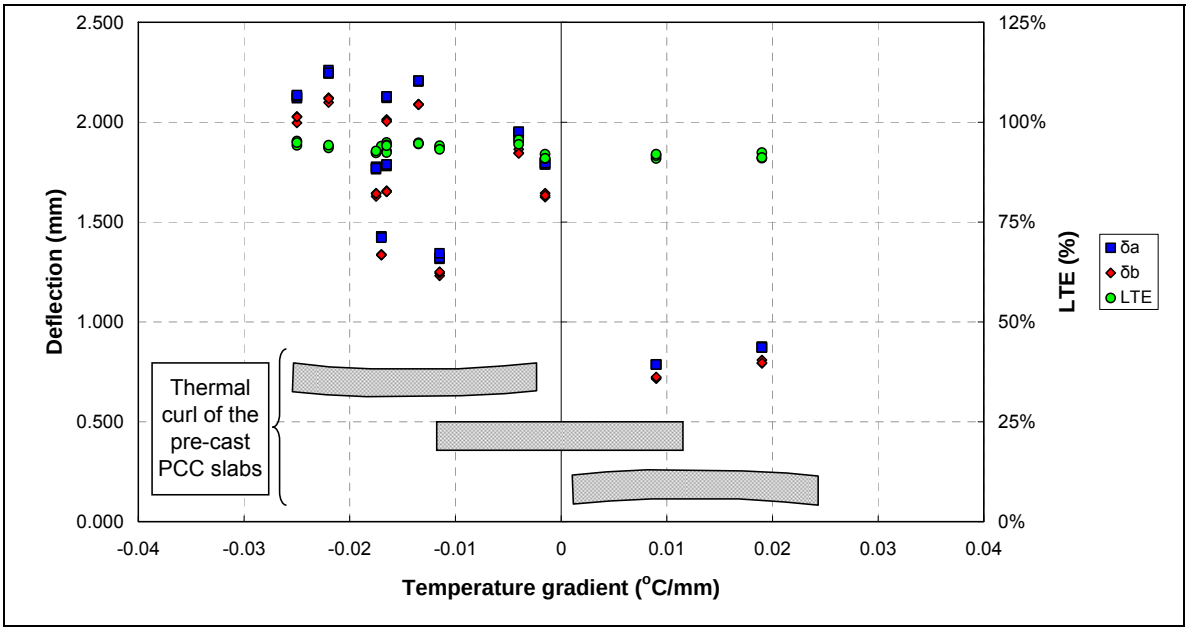

Figure 21: Final JDMD deflection and LTE data for JDMDs 1 and 2 at the 60 kN deflection load plotted against the slab temperature gradient.

The JDMD deflection data indicates substantial change in the structural condition of the pavement, with the deflection increasing from about 0.5 mm to 2.0 mm at a temperature gradient of -0.02°C/mm and increasing from about 0.25 mm to 0.8 mm at a temperature gradient of +0.02°C/mm. This agrees well with the observations from the

MDD data. The JDMD LTE data do not show the same temperature gradient dependency as the MDD LTE data and remained in a range between 80 and 100 percent for the duration of Test 597FD. However, the JDMD LTE data again show no deterioration in the LTE for the duration of Test 597FD as was the case with the MDD LTE data.

2.4.2 Conclusions Drawn from JDMD Data

The following conclusions are drawn from the vertical JDMD deflection data at the transverse joints of Section 597FD:

- The magnitude of the JDMD deflection depends on the magnitude of the deflection load, with a higher deflection load causing a higher deflection. The peak deflection at the cabin-end transverse joint increased at about 850,000 load repetitions without any increase in the deflection or traffic loads. This coincides with the full development of the corner cracks at the cabin-end transverse joint at 844,000 repetitions (refer to Table 3 and Figure 5). This increase in deflection did not occur at the tow-end transverse joint where no corner crack developed.
- Daily temperature changes in the pre-cast PCC slab cause a temperature gradient in the slab that affects the peak JDMD deflection, with the peak JDMD deflection increasing at negative temperature gradients.
- Section 597FD exhibits some structural change evidenced by a substantial increase in the peak 60 kN deflection from the start to the end of the test.
- The JDMD-based LTE at the transverse joints did not deteriorate at all during the HVS test on Section 597FD.

2.5 Horizontal JDMD data for Test 597FD

Horizontal JDMD data were collected according to the schedule shown in Table 2 at the horizontal JDMD locations shown in Figure 2. The horizontal JDMDs of main concern are JDMDs 13 and 14 mounted across the cabin- and tow-end transverse joints respectively. Figure 22 shows a typical example of the transverse joint activity recorded by JDMDs 13 and 14. Joint activity is term used to describe chances in horizontal displacement measured across the joint, i.e opening and closing of the joint.

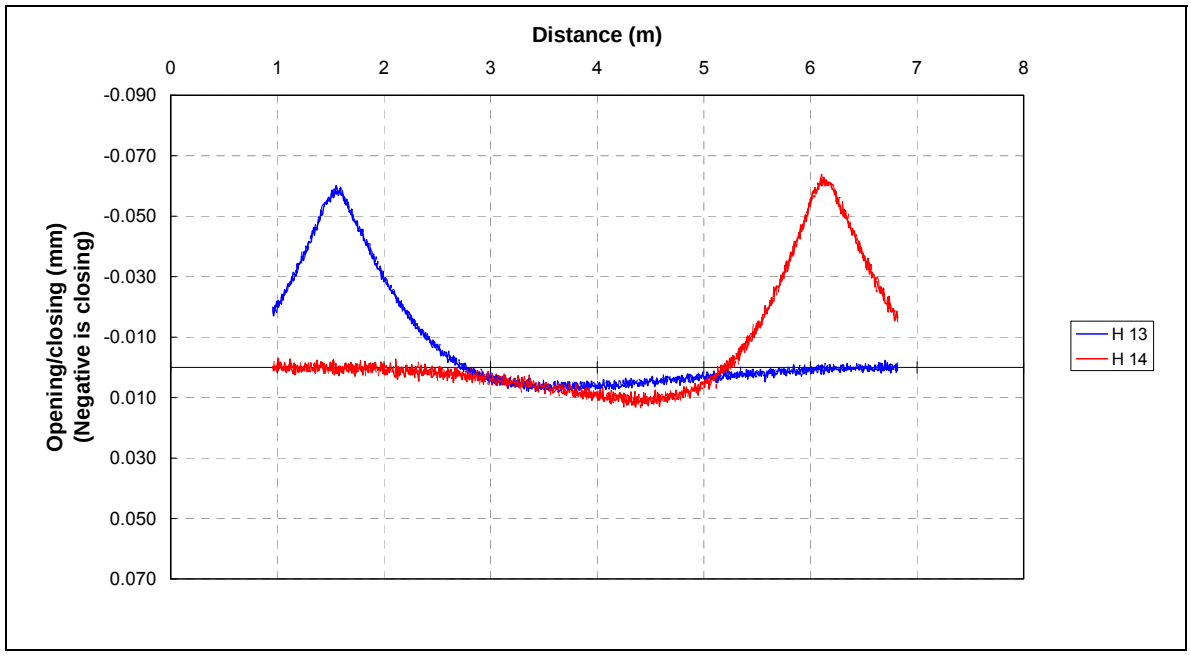

Figure 22: Typical transverse joint activity result from JDMDs 13 and 14.

A summary of the opening, closing, and total joint activity for the cabin- and tow-end transverse joints are shown in Figure 23 and Figure 24 respectively for the 60 kN deflection load.

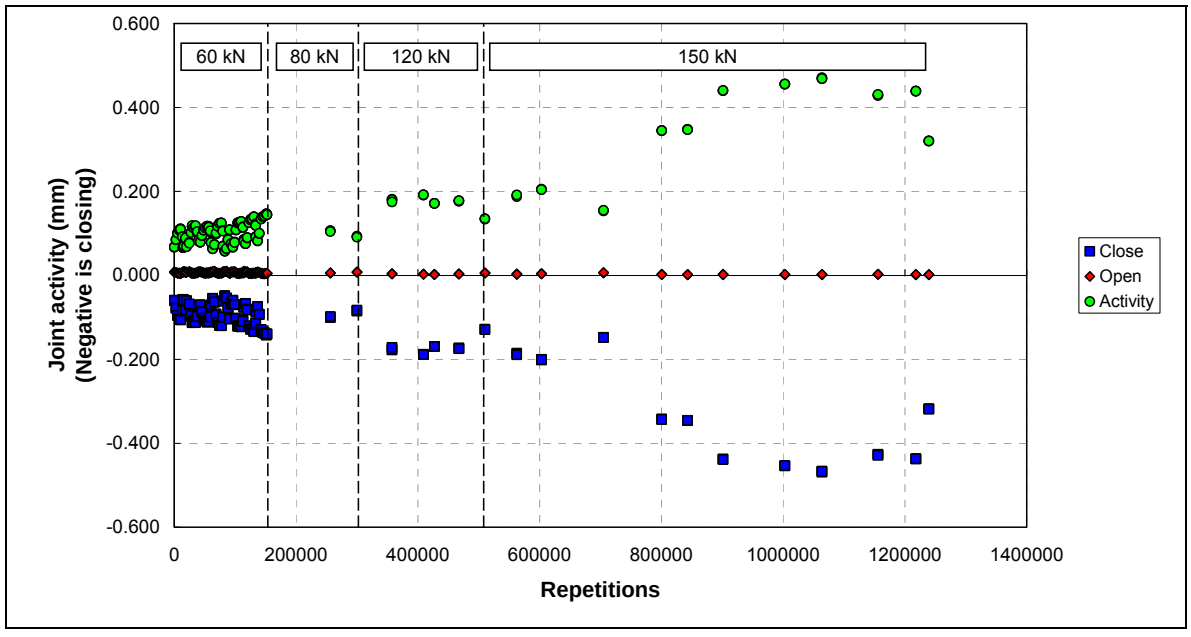

Figure 23: 60 kN joint activity of the cabin-end transverse joint recorded by JDMD 13.

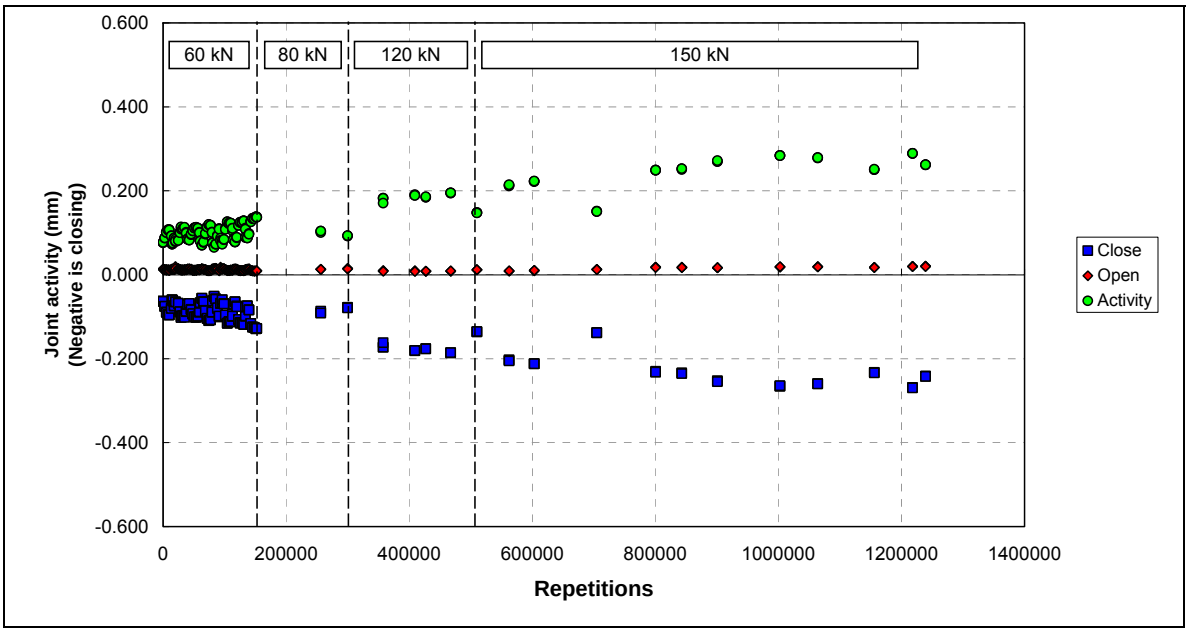

Figure 24: 60 kN joint activity of the tow-end transverse joint recorded by JDMD 14.

There is a gradual increase in the 60 kN joint activity at both JDMDs with increasing load repetitions but a substantial increase in the joint activity occurred at JDMD 13 where the corner crack developed beyond 800,000 repetitions. The joint activity was therefore plotted against the temperature gradient of the slab for the initial conditions (<100,000 repetitions), the pre-cracked phase of the 150 kN trafficking portion of the test (300,000 to 800,000 repetitions) and the post-cracked portions of the 150 kN trafficking portion of the test (800,000 repetitions to the end of the test). The results from this process are shown in Figure 25 for JDMD 13 at the cabin-end transverse joint where the crack occurred and in Figure 26 for JDMD 14 at the tow-end transverse joint where no crack occurred.

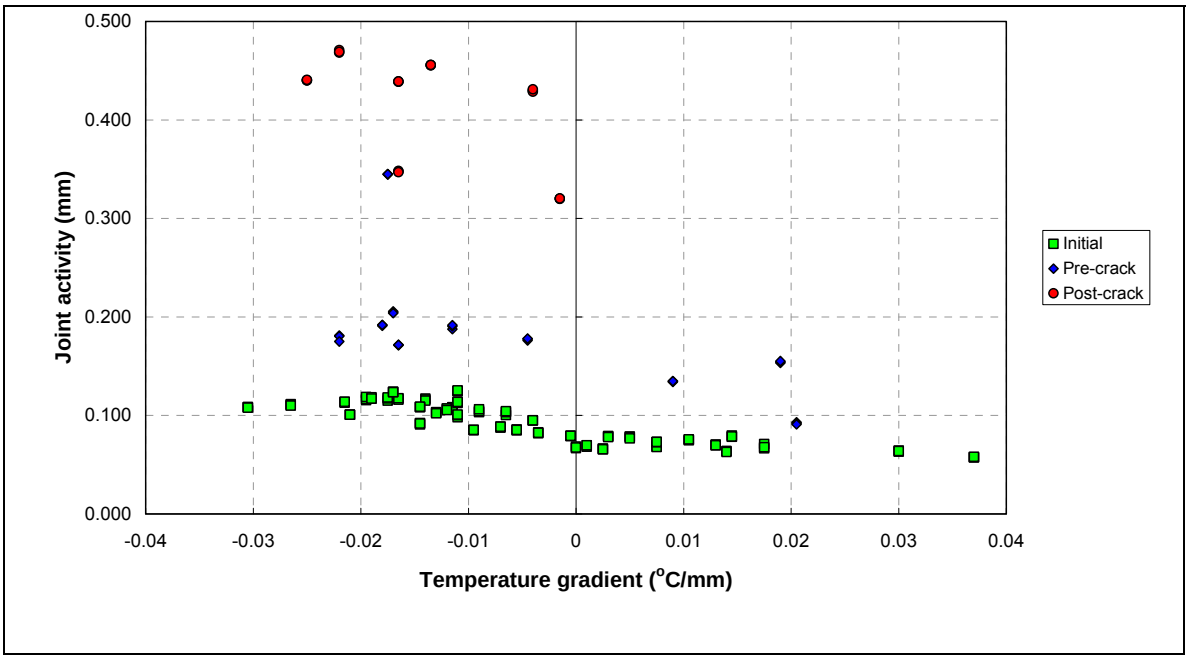

Figure 25: Joint activity of the cabin-end transverse joint recorded by JDMD 13 plotted against the temperature gradient of the slab.

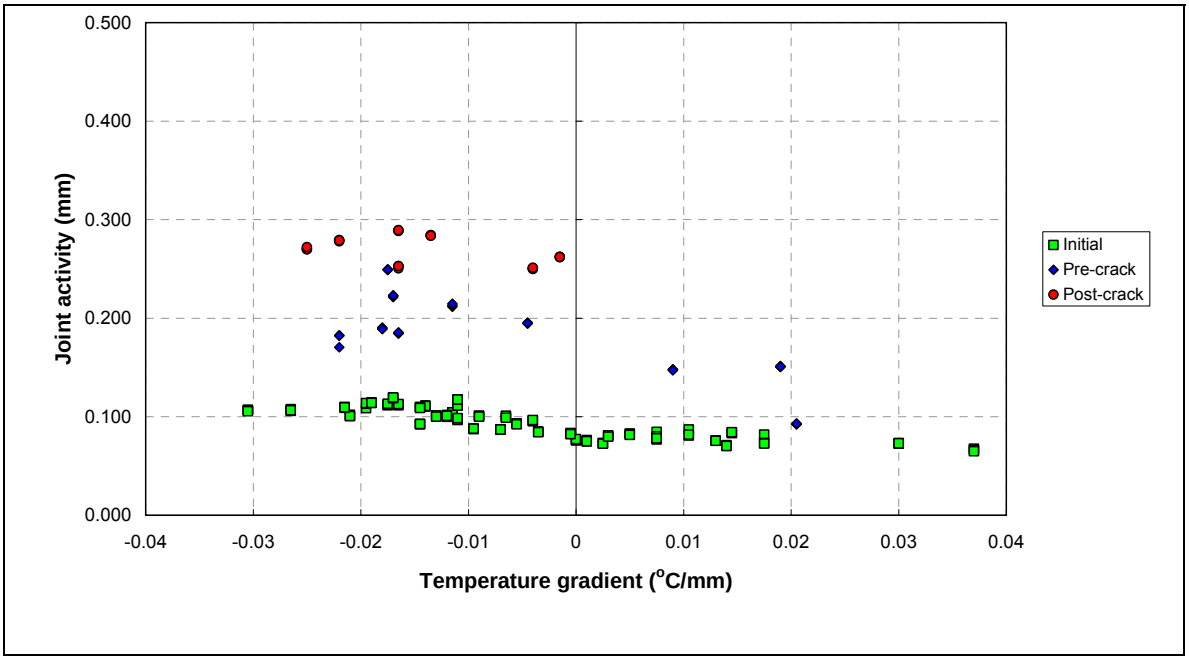

Figure 26: Joint activity of the tow-end transverse joint recorded by JDMD 14 plotted against the temperature gradient of the slab.

There is a substantial difference in the joint activity of the two transverse joints with the joint activity increasing significantly at the transverse joint where the corner crack developed.

The following conclusions are drawn from the horizontal JDMD joint activity data at the transverse joints of Section 597FD:

- The joint activity at the cabin-end transverse joint increased at about 800,000 load repetitions without any increase in the deflection or traffic loads. This coincides with the full development of the corner cracks at the cabin-end transverse joint at 844,000 repetitions (refer to Table 3 and Figure 5). This increase in joint activity did not occur at the tow-end transverse joint where no corner crack developed.
- Daily temperature changes in the pre-cast PCC slab cause a temperature gradient in the slab that affects the joint activity, with the joint activity increasing at negative temperature gradients. This temperature dependency of the joint activity becomes more evident than at the beginning of the test.

2.6 Structural Capacity of Section 597FD

A number of factors need to be noted in terms of the assessment of the structural capacity of the pre-cast PCC pavement at the San Bernardino test site based on the HVS test data. As stated in the Introduction, the support conditions of the test pavement were probably better than would be expected on normal rehabilitation projects; the environmental conditions were optimal during the test, with no water applied to the test section; and the construction was well controlled.

In addition to this, the initial HVS test was not run until full structural failure occurred. The slab corners on either side of the cabin-end transverse joint developed full corner cracks. Some structural damage did occur, with the peak MDD and JDMD deflection increasing from about 0.5 mm to between 1.5 and 2 mm at negative slab temperature gradients. At a positive slab temperature gradient the deflection increased from about 0.25 mm to values between 0.8 and 1.0 mm. The LTE of the grouted dowel joints, which was anticipated to reduce rapidly under the HVS test, held up exceptionally well and showed no deterioration throughout the test.

The only tangible distress that occurred was the development of the corner crack at the cabin-end transverse joint which was first observed at 762,044 repetitions of mixed traffic. This condition, representing a case where 50 percent of the transverse joints have corner cracks (one transverse joint on the HVS section cracked, the other did not) is an

indicator of the structural capacity of the pavement. It is, however necessary to convert the mixed traffic to its equivalent standard axle (ESAL) value to interpret the result.

The conversion of the 80, 120, and 150 kN load repetitions to an ESAL value is done with the AAHSTO damage law but because of uncertainty regarding the AASHTO damage power, a Monte Carlo type of simulation was done by randomly generating 1000 AASHTO damage power values according to a normal distribution with a minimum value of 3.8, an average of 4.2, and a maximum value of 4.6. These AASHTO damage power values were then used to convert the mixed traffic at the time when the corner crack was first observed to its ESAL value. The result from this process is shown in Figure 27. The mode of the distribution (the bin of values with the highest frequency) was between 80 and 90 million ESALs. In a design case of an important highway it is advisable to use the 10^{th} percentile of the distribution to ensure that 90% of all observations actually exceed the design target. The 10^{th} percentile value of the distribution in Figure 27 falls between 70 and 80 million ESALs. This value exceeds the design traffic target of 40 million ESALs, but it must be emphasized again that the test was performed under favorable conditions.

The test pavement was also simulated with *cncPave3.19,* a rigid pavement design software package used in South Africa. This analysis indicated a distribution of ESALs from 40 to 100 million for a condition where 50 percent of the slabs were cracked. The distribution from this analysis therefore lies slightly offset to the left of the distribution shown in Figure 27, but also indicates that given the favorable conditions under which the HVS test was done, the structural capacity to a condition where 50 percent of the transverse joints exhibits corner cracks would be expected to exceed the design traffic target of 40 million ESALs.

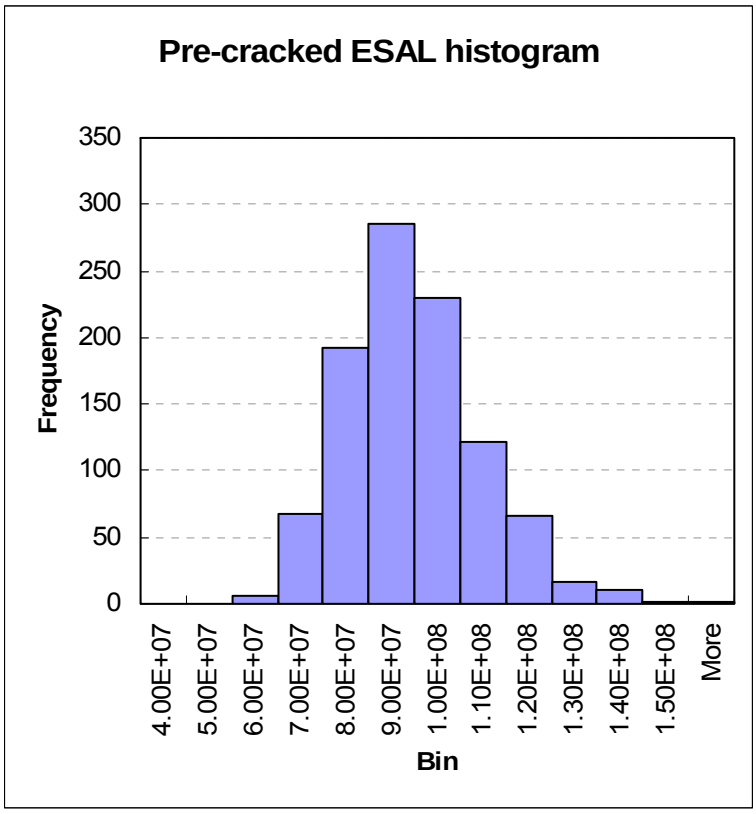

Figure 27: Distribution of ESALS for a condition of corner crack initiation at 50 percent of the transverse joints.

3. INTERIM CONCLUSIONS

The following interim conclusions are made subject to the provisions that the support conditions of the test pavement are probably better than would be expected on normal rehabilitation projects; the environmental conditions were optimal during the HVS test, with no water applied to the test section; and the construction was well controlled:

- Deterioration of the pre-cast PCC pavement system did occur during the HVS test in terms of a significant increase in the deflection of the pavement. However, this increase in deflection did not result in any terminal failures of the pavement during the HVS test.
- The process of grouting the dowel bars seems to be effective based on high load transfer between slabs that was maintained under fairly aggressive loading conditions during the HVS test.
- Although corner cracking occurred on both sides of one of the transverse joints on the HVS section, the pavement was not yet in a terminal condition at the time when the initial HVS test was stopped. It is strongly recommended that future HVS testing should be conducted by adding water to the test section to investigate the possible erosion and pumping of the grouted bedding material at the PCC/CTB interface that may result in step-faulting of the pavement.

Therefore, the main conclusion of this tech memo is that — given the design of the pre-cast PCC pavement tested at the San Bernardino test site, the tight control over the construction process, and the favorable HVS test conditions — premature failure is not anticipated with the use of the pre-cast PCC pavement on actual rehabilitation projects. It is understood that the ultimate structural capacity of the system will be influenced by many factors excluded from the initial HVS tests. The structural capacity of the system will have to be determined for a range of support and environmental conditions before it can be used with higher confidence. However, based on the conditions and performance of Test 597FD, it is expected that the pre-cast panels will meet and probably will exceed the design traffic of 40 million ESALs.

4. REFERENCES

1. Partnered Pavement Research Program (PPRC). (March 2005) *HVS Test Plan: Super-Slab Reconstruction of Rigid Pavement Sections.* (UCPRC-TP-2005-01)

2. Kohler, E., Theyse, H., and du Plessis, L. (2007) *Construction and Preliminary HVS Tests of Pre-Cast Concrete Pavement Slabs.* (UCPRC-RR-2006-10).